MATERIALS SCIENCE AND TECHNOLOGY
https://doi.org/10.1080/02670836.2021.2007455

Enriching mean-field self-consistent texture simulations using the full-field FFT model

Mirtunjay Kumar[a], Amit Singh[a] and Sumeet Mishra[b]

[a]Department of Materials Science and Engineering, Indian Institute of Technology Kanpur, Kalyanpur, Kanpur, India; [b]Department of Metallurgical and Materials Engineering, Indian Institute of Technology Roorkee, Roorkee, India

ABSTRACT

In the present work, crystal plasticity simulations using the fast Fourier transform (FFT) based Düsseldorf advanced material simulation kit (DAMASK) are performed to provide new insights on choosing the value of interaction parameter in the localisation equation of the visco-plastic self-consistent (VPSC) model. A statistical criterion based on the distribution of shear rates ($\dot{\gamma}_s$) at each material point is obtained using DAMASK, which enables the judicious selection of the interaction parameter in the VPSC model. Subsequent large-scale texture simulations via VPSC indicated an excellent match between experimental and simulated textures, which establishes the effectiveness of the proposed approach of learning from full-field models and using it in the mean-field, less computationally expensive VPSC model for performing efficient texture simulations.

ARTICLE HISTORY
Received 26 July 2021
Revised 12 November 2021
Accepted 13 November 2021

KEYWORDS
Crystal plasticity; crystallographic texture; DAMASK; VPSC

Introduction

Since the development of the seminal Taylor–Bishop–Hill (TBH) theory in 1951, texture simulations have found widespread use in the materials mechanics community to understand the deformation response of a wide class of materials [1,2]. The initial simulations were mostly performed for high symmetry cubic materials, followed by an adaptation of the theory for low symmetry hexagonal materials [3–5]. It was observed that full constraint TBH theory provided a decent qualitative prediction of the texture evolution in cubic materials. However, several drawbacks were observed when the TBH theory was used for quantitative texture predictions in cubic materials. Some of the key drawbacks were too sharp or strong simulated texture and a mismatch in Euler space with respect to the position of Copper component ($\varphi_1 = 90°, \varphi = 35°, \varphi_2 = 45°$) [6,7]. The Taylor model usually predicts the Dillamore component ($\varphi_1 = 90°, \varphi = 27°, \varphi_2 = 45°$) which is 8° away from the ideal copper component. Other drawbacks of the full constraint TBH theory were fast evolution of simulated texture, the ambiguity in the choice of active slip systems and the wrong balance of the texture components copper, S ($\varphi_1 = 59°, \varphi = 37°, \varphi_2 = 63°$) and brass ($\varphi_1 = 35°, \varphi = 45°, \varphi_2 = 0°$) along the β fibre [6,7]. All of these drawbacks were traced back to the basic assumption of the TBH theory that individual grains in a polycrystalline aggregate undergo the same amount of deformation and change in shape as the entire polycrystal [8].

Based on experimental evidence, it was observed that the assumptions in the TBH theory were 'too strict' and that individual grains can undergo different amounts of strain or shape changes depending on the mutual interactions with neighbouring grains [9,10]. Therefore, several new models have been developed over the years that have abandoned the strict constraints imposed by the TBH model and have also incorporated grain interactions to improve the quality of texture prediction. To name a few, the visco-plastic self-consistent (VPSC) model and advanced LAMEL type models (ALAMEL) were developed by Molinari et al. [11], Lebensohn and Tome [12] and Van Houtte et al. [13]. The VPSC model considers long-range interaction of individual grains with the homogenous equivalent medium (HEM), while ALAMEL model considers local interactions at the grain boundaries by maintaining continuity conditions across the grain boundaries. Compared to the TBH model, these mean-field models have shown a significantly improved performance in terms of texture development and anisotropy prediction [14–16]. In the past two decades, other models such as the crystal plasticity fast Fourier transform (CPFFT) method and the crystal plasticity finite element (CPFEM) method have also been developed, in which grain interactions

CONTACT Sumeet Mishra sumeet.mishra@mt.iitr.ac.in Department of Metallurgical and Materials Engineering, Indian Institute of Technology Roorkee, Roorkee 247667, India

Supplemental data for this article can be accessed here. https://doi.org/10.1080/02670836.2021.2007455

and the local stress and strain fields can be adequately accounted for by using a sufficiently fine mesh resolution [17,18]. The CPFEM and CPFFT models solve for stress equilibrium and strain compatibility and provide important insights into the spatial variation of properties and the local distribution of micromechanical fields [19].

However, these full-field CPEFEM and CPFFT models are computationally intensive and therefore require high-end computational resources. Therefore, full-field crystal plasticity simulations on the component scale are currently not computationally feasible. On the other hand, mean-field models such as VPSC are computationally efficient (super-fast) and can be integrated into a large-scale engineering model. The efficient nature of the VPSC model makes it the most extensively used model for performing texture simulations when compared to the full-field models. The VPSC model has shown good predictive capabilities for cubic materials with high symmetry and hexagonal materials with low symmetry by integrating different twin modes [20]. Considering the usefulness of the VPSC model, several strategies have been tried to incorporate more material physics into the VPSC model, such as n-site VPSC [21,22], dislocation substructure-based hardening laws [5] and mechanical threshold stress model [23], without compromising on the computational efficiency.

One of the key parameters in VPSC, which controls the simulation texture, active slip systems, yield locus and anisotropy in the *R*-value, is the interaction parameter 'α' [11,24]. By using different values of 'α' that vary between zero and infinity, several material deformation conditions can be mimicked, the extremes being the uniform stress state ($\alpha = 0$, static model) and the uniform strain state ($\alpha = \infty$, the Taylor model). It should be noted that VPSC also includes the secant and tangent interaction schemes where the α parameter is 1 and m, respectively, where m is the rate sensitivity exponent in the power law for slip [25]. In addition, the interaction between the grains and the surrounding homogeneous equivalent medium (HEM) is also dependent on the α parameter. Complete details on the grain–HEM interaction and the different values of α parameter (finite element tuned, etc.) can be found in Tomé [25].

Recently, several simulation studies were carried out in the VPSC framework to predict texture evolution. For instance, Mishin et al. [26] performed VPSC simulations to understand the deformation mechanism and texture evolution in beryllium during rolling at room temperature. Mishin et al. [26] invoked both slip and twinning deformation modes and observed that basal slip has the maximum contribution towards texture development. Mishin et al. [26] used $\alpha = 0.1$ to achieve the best possible agreement between experimental and simulated textures. Roatta et al. [27] performed VPSC simulations to predict the texture evolution during monotonic loading of the Zn–Cu–Ti alloy, using the affine interaction scheme to reproduce the experimental results. Roatta et al. [27] suggested that affine interaction leads to predictions that lie between the secant and tangent approaches for high non-linearity and are therefore best suited for hexagonal materials. The VPSC model has also been extended to novel high entropy alloys. Kaushik et al. [28] carried out simulations to understand the classical texture transition from the copper type to brass type during cold rolling of high entropy alloys. Similar studies were also performed by Tazuddin et al. [29] to understand texture evolution in single-phase f.c.c high entropy alloys. Tazuddin et al. [29] invoked the conventional $\{111\}\langle 1\bar{1}0\rangle$ slip and $\{111\}\langle 11\bar{2}\rangle$ partial slip along with the tangent interaction scheme in order to capture the texture evolution in high entropy alloys. Saleh et al. [30,31] have systematically investigated texture evolution during plane strain compression and uniaxial tension of twinning induced plasticity steels (TWIP). The α parameter chosen by Saleh et al. [30,31] was 0.05, viz. the tangent interaction scheme to achieve a close proximity between experimental and simulated textures. Texture evolution in b.c.c. materials such as low carbon steel was recently discussed by Takajo et al. [32] to understand the governing mechanism behind the highly developed alpha fibre and a weak gamma fibre. Takajo et al. [32] performed VPSC simulations with all the available interaction schemes such as Taylor, secant, intermediate and tangent. Based on the comparison between experimental and simulated textures, Takajo et al. [32] decided the α parameter.

Aside from the brief overview of using the α parameter in the section above, there are several studies in the literature that use the α parameter as a fitting tool to get the best match between experimental and simulated textures. To the best of our knowledge, there are no methods available in the literature to determine the α parameter a priori before running the VPSC simulations.

Given the importance of the α parameter, there should be a reasonable way to choose its value. In this regard, the present article aims to enrich the mean-field VPSC model by providing insights into the selection of the α parameter value using small-scale full-field CPFFT simulations. In the broadest sense, this article aims to highlight the findings from small-scale full-field CPFFT simulations over a representative volume element (RVE) that can be used to perform efficient and transparent texture simulations via VPSC.

Material and methods

In the present work, an Al–Mg–Si alloy with the composition (in wt.%) 97.6Al–0.7Si–1Mg–0.3Cu–0.2Fe–0.17Cr–0.04Mn was chosen as a model material to investigate texture evolution. The samples were solution

treated at 823 K for 1 h, followed by rapid quenching in cold water to retain the single-phase supersaturated solid solution at room temperature. The solution-treated samples were then cold rolled up to 90% reduction in thickness in multiple steps (23) with each step corresponding to a strain increment of 0.1. The texture of the rolled samples was then measured at the mid-thickness level to avoid the friction and shearing effect of the rolls. Four incomplete pole figures (111), (200), (220) and (311) were measured with a maximum tilt angle of 75° and rotation of 360°. The measurements were performed using Ultima IV, Rigaku which was operated with 40 kV voltage and 40 mA current. The defocusing corrections were carried out before constructing the orientation distribution function (ODF) using the freely available open-source software package MTEX [33]. The ghost correction option in MTEX was also invoked while computing the ODF.

Modelling and simulations

Full-field crystal plasticity formulism

In the present work the Düsseldorf Advanced Material Simulation Kit (DAMASK) [34–36] based on a spectral solver was used to carry out full-field simulations (homogenisation = none) and learn about the choice and the number of active slip systems during plane strain rolling deformation. A brief overview of the constitutive model is given in the following section, followed by simulation procedure and hardening parameters in the next section.

Crystal plasticity constitutive model

At the heart of the constitutive model is the multiplicative decomposition of deformation gradient (F) into elastic (F_e) and plastic components (F_p).

$$F = F_e F_p \tag{1}$$

The velocity gradient tensor (L_p) can be subsequently written as

$$L_p = \dot{F}_p {F_p}^{-1} \tag{2}$$

Since plastic deformation takes by crystallographic slip, the velocity gradient L_p can also be written as

$$L_p = \sum_{\alpha} \dot{\gamma}^{\alpha} (b^{\alpha} \otimes n^{\alpha}) \tag{3}$$

Here, $\dot{\gamma}^{\alpha}$ is the shear rate on the slip system α, n is the slip plane normal and b is the slip direction. The slip directions and planes normal are defined in relation to the initial (reference) configuration. Since lattice directions are preserved in the intermediate configuration, they are therefore the same as in the initial configuration. Considering the rate-sensitive constitutive law, $\dot{\gamma}^{\alpha}$ (in terms of second Piola–Kirchhoff stress) is given by,

$$\dot{\gamma}^{\alpha} = \dot{\gamma}_0 \left| \frac{\tau^{\alpha}_{RSS}}{\tau^{\alpha}_{CRSS}} \right|^{1/m} \mathrm{sgn}(\tau^{\alpha}_{RSS}) \tag{4}$$

Here, $\dot{\gamma}_0$ is the reference strain rate, τ^{α}_{RSS} is the resolved shear stress and τ^{α}_{CRSS} is the critical resolved shear stress (CRSS) of the slip system α and m is related to strain rate sensitivity ($m = 1/20 = 0.05$). The hardening of slip systems or the rise in CRSS is due to shear on all the slip systems and can be expressed as

$$\tau^{\alpha}_{CRSS} = \tau_0 + \sum_{\beta} H_{\alpha\beta} |\dot{\gamma}^{\beta}| \tag{5}$$

Here, τ_0 is the initial slip resistance and $H_{\alpha\beta}$ is the hardening matrix which represents interaction between different slip systems. Typically, $H_{\alpha\beta}$ is expressed as

$$H_{\alpha\beta} = q_{\alpha\beta} \times h^{\beta}_0 \left(1 - \frac{\tau^{\beta}_{CRSS}}{\tau^{\beta}_{sat}} \right)^{a} \tag{6}$$

Here, $q_{\alpha\beta}$ is the symmetric hardening matrix which expresses the interaction between slip systems, h_0 is the initial hardening rate, τ_{sat} is the saturation stress and a is the hardening exponent. It should be noted that the material flow behaviour can be represented by specifying hardening parameters τ_0, h_0, τ_{sat} and a.

DAMASK pre- and post-processing

The first step in pre-processing for DAMASK simulations is to generate a RVE. Since DAMASK simulations are computationally expensive, it is not possible to run large-scale texture simulations with almost 10,000 grains. However, several important information about the deformation response of the material can be obtained by performing DAMASK simulations over an RVE, which can then be subsequently used in the VPSC environment to perform efficient and transparent texture simulations. In the present work, we have used the initial texture data of the solution-treated sample to prepare the RVE. Firstly, the function 'seeds_fromRandom' was used to place 150 random seeds into a grid of dimensions $512 \times 512 \times 1$. The dimension along 'Z-direction' was restricted to reduce the computational demand. The experimentally measured texture of the solution-treated sample was then discretised using the widely used MATLAB toolbox MTEX to produce 150 single orientations (Euler angles). The single orientations were then placed in the existing 'seed file'. Finally, using a Voronoi tessellation, the seed positions and the orientations were combined to produce a discretised RVE. The discretised RVE was then visualised using the open-source Paraview software.

After preparing the RVE, the next step in pre-processing is to specify the elastic and plastic properties and the deformation conditions. The various elastic

Table 1. Elastic and hardening parameters used for DAMASK simulations.

Parameters	Values
C_{11}	106 GPa
C_{12}	61 GPa
C_{44}	28 GPa
$\dot{\gamma}_0$	0.001 s^{-1}
τ_0	30 MPa
τ_{sat}	118 MPa
h_0	370 MPa
a	2

and plastic properties which are required for running DAMASK simulations are specified in Table 1. The deformation condition was specified by imposing the velocity gradient which can be expressed as

$$L_{ij} = \begin{bmatrix} L_{11} & 0 & 0 \\ 0 & 0 & 0 \\ 0 & 0 & L_{33} \end{bmatrix} \quad (7)$$

For plane strain deformation, we generally have $L_{11} = -L_{33}$. The simulations were performed in 2300 incremental steps, with each step corresponding to a strain increment of 0.001. The total cumulative strain was $\varepsilon = -2.3$ that corresponds to 90% rolling reduction. Following the simulations, the post-processing and data visualisation were performed using DREAM 3D, Paraview and MATLAB [37].

Visco-plastic self-consistent simulations

The visco-plastic self-consistent (VPSC) model is a mean-field model where a grain is considered as an inclusion embedded in a HEM [12,38]. As a result, the VPSC model considers long-range interaction between the individual grains and the HEM matrix. On the other hand, DAMASK is a full-field model where local grain interactions are accounted for during simulations. However, DAMASK simulations are computationally expensive and cannot be used to run large-scale simulations with nearly 10,000 grains, which is generally required for the accurate prediction of texture evolution and plastic anisotropy. In this scenario, the VPSC model represents the best possible compromise between the detailed and computationally demanding DAMASK model and the preliminary Taylor-type models. At the heart of the VPSC model is the following localisation equation where different types of deformation patterns can be mimicked by controlling the interaction parameter 'α'.

$$s^g - S = \alpha(\Gamma^{sgg\,-1} + A^s)(d^g - D) \quad (8)$$

Here, s^g and d^g are grain level stress state and strain rate tensors, while S and D are the macroscopic stress state and strain rate tensors. A^s is the secant modulus (4th rank tensor) which controls the behaviour of HEM and relates the macroscopic stress with macroscopic strain rate. Γ^{sgg} is also a 4th rank tensor which is related to the shape and orientation of the grain. As can be observed from the above equation, for $\alpha = \infty$, $d^g = D$, viz. upper bound full constraint Taylor condition. For $\alpha = 0$, $s^g = S$ which is the lower bound static condition. Apart from the extreme values of α, the VPSC model also includes other values of α such as 1 (secant), $1 < \alpha < m$, e.g. $\alpha = m/2$ (intermediate) and m (tangent). Note that in the present calculations $m = 0.05$. For $\alpha = 1$, conditions very close to the Taylor model are approached, suggesting that stresses are very different in the individual grains while the strain rates are more or less equal. For $\alpha = 0.05$, the opposite end of the spectrum, viz. the static condition is approached, where the stresses are equal, but the strains or strain rates are very different in the individual grains.

As can be envisioned from the previous paragraph, the texture simulation via the VPSC model is very sensitive to the choice of the α parameter. The direct influence of the choice of the α parameter is on the number of active slip systems, which in turn is known to be the decisive factor in controlling the texture evolution. So, there is a need to develop a fundamental approach for selecting the value of the α parameter. To the best of our knowledge, VPSC simulations have been performed so far by tuning the value of the α parameter so that a reasonable match between experimental and simulated textures can be achieved. In this context, we have performed DAMASK simulations to learn about the distribution of the shear rates on the individual slip systems, which in turn enables us to decide the α parameter in the subsequent VPSC simulations.

To perform VPSC simulations, bulk texture data of the solution-treated sample was discretised to generate 10,000 individual orientations, which were then used as input into the VPSC code. The same hardening parameters (τ_0, h_0, τ_{sat} and a) which were used in DAMASK simulations were also used to run VPSC simulations. The velocity gradient given in Equation (7) was imposed to mimic the rolling deformation condition. The simulations were performed up to a total strain level of $\varepsilon = -2.3$ which is equivalent to the 90% rolling reduction. The strain increment per step was kept at 0.001. It should be noted that VPSC ignores elasticity, while elasticity is taken into account in DAMASK. However, since the study involves large plastic strains, the effect of elasticity would be minimal.

Results and discussion

The texture of the solution-treated material represented via important ODF sections ($\varphi_2 = 0°, \varphi_2 = 45°, \varphi_2 = 65°$) is given in Figure 1(a). It is clear from the ODF sections that the solution-treated sample shows a classical {100}⟨001⟩ cube texture, which is generally observed in aluminium alloys after recrystallisation

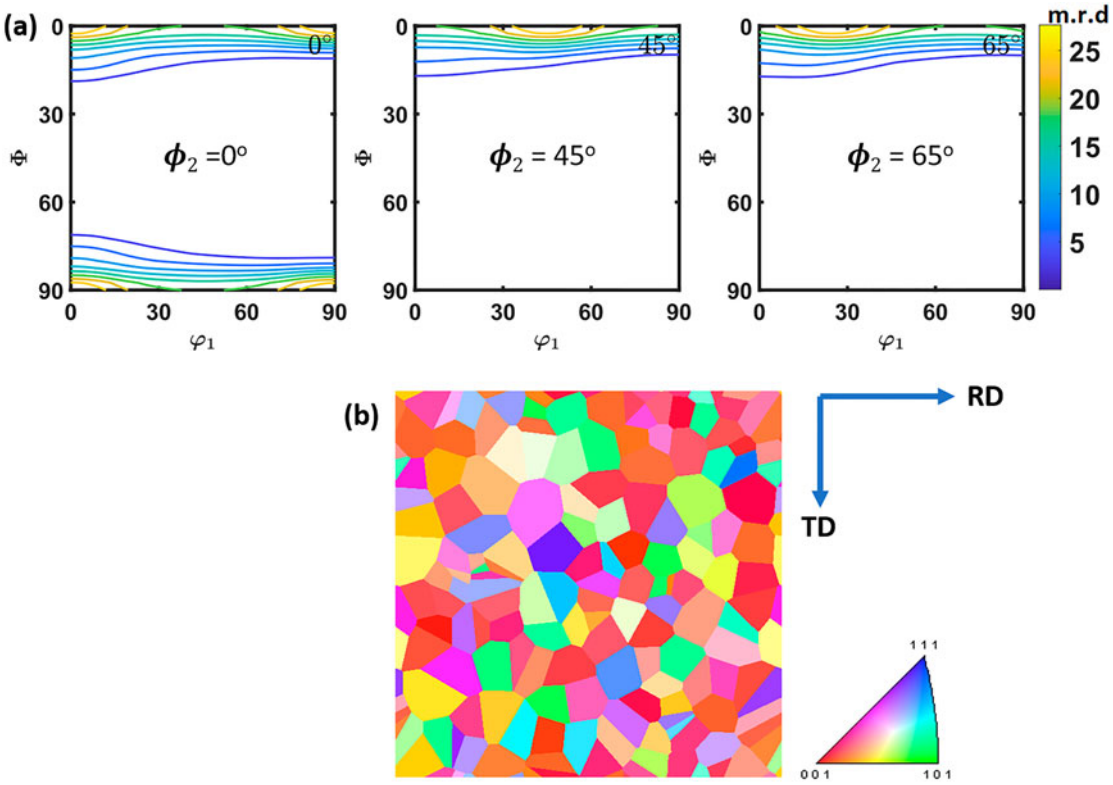

Colour online, B/W in print

Figure 1. (a) Initial texture of the solution-treated sample and (b) representative volume element for DAMASK simulations prepared from the initial texture.

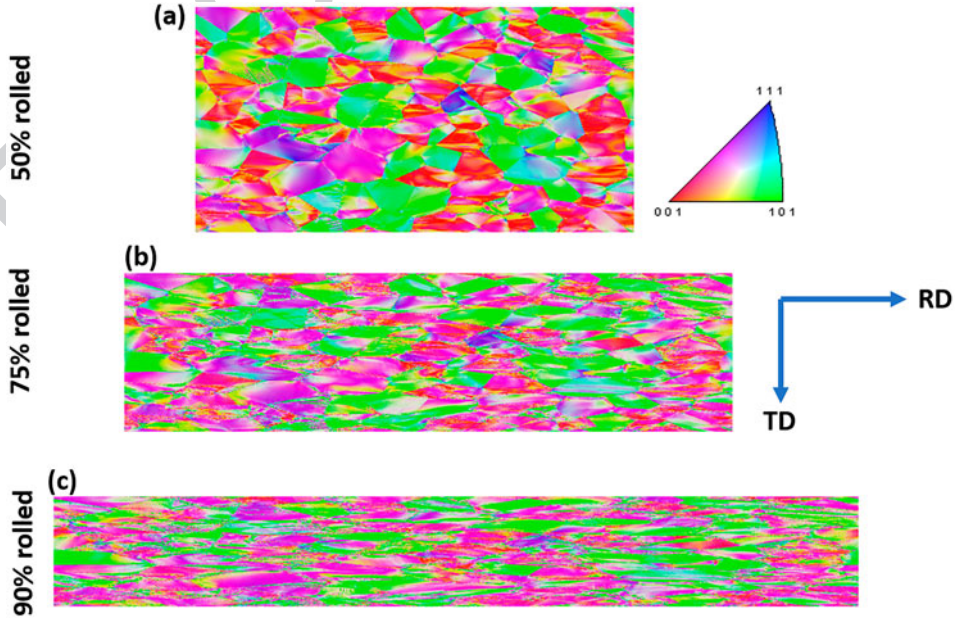

Colour online, B/W in print

Figure 2. Simulated inverse pole figure maps (IPF Z) after different rolling reductions: (a) 50% ($\varepsilon = 0.69$), (b) 75% ($\varepsilon = 1.4$) and (c) 90% ($\varepsilon = 2.7$).

annealing [39]. The texture is fairly sharp with a maximum intensity of 25 m.r.d. As mentioned previously, the cube texture was discretised to produce 150 single orientations, which were then used to generate the representative volume element (Figure 1(b)) with dimensions of $512 \times 512 \times 1$. This RVE was used as input in DAMASK to carry out the simulations up to a cumulative strain of $\varepsilon = -2.3$.

Figure 2 shows the simulated normal direction inverse pole figure (IPF) maps at different levels of strain. As is generally observed in the case of rolling deformation, the individual grains tend to be flattened and elongated, viz. pancake-shaped with increasing rolling reduction. In addition, the presence of deformation heterogeneity in relation to intragranular orientation gradients can be clearly observed in the simulated

Colour online, B/W in print

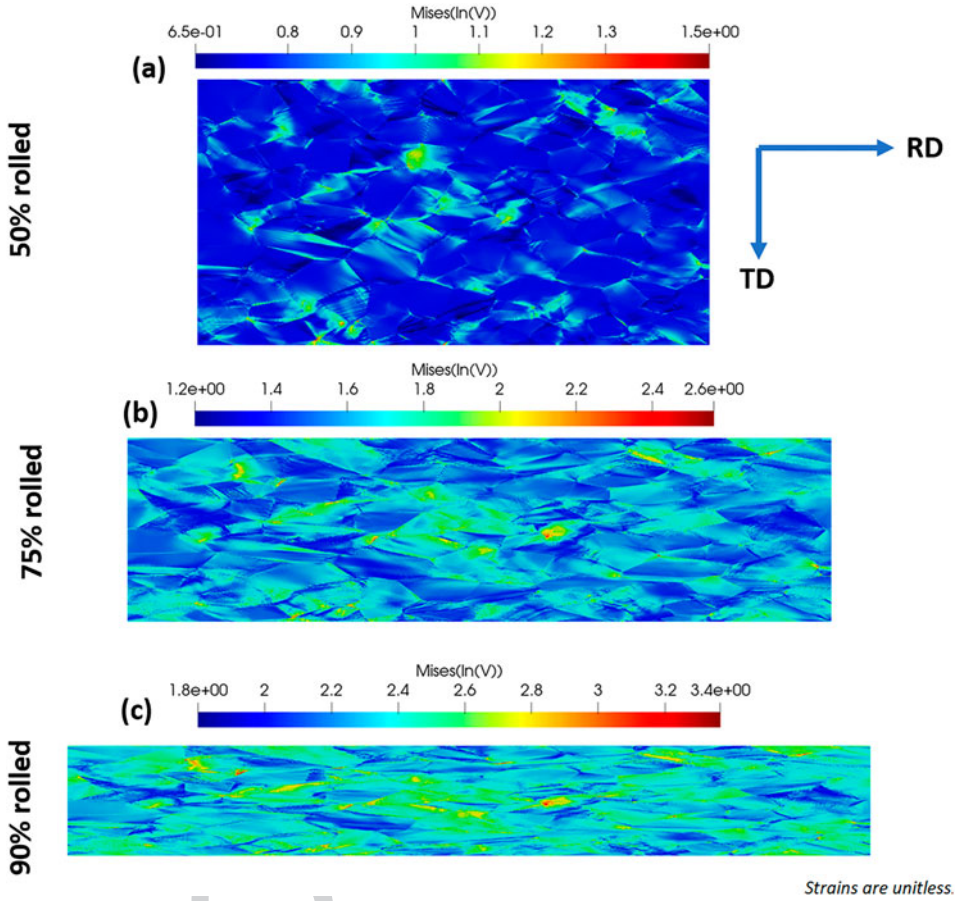

Figure 3. Spatial distribution of Von-Mises' equivalent strain after different rolling reductions: (a) 50% ($\varepsilon = 0.69$), (b) 75% ($\varepsilon = 1.4$) and (c) 90% ($\varepsilon = 2.7$).

IPF maps. The presence of intragranular orientation gradients provides the immediate information that Taylor-type deformation pattern of uniform strain state is not followed. Further insights regarding deformation behaviour can be obtained by analysing the spatial distribution of equivalent strain and stress (Figures 3 and 4). It can be observed that the actual deformation response of the material is far away from both uniform stress and strain state. There is indeed significant variation in equivalent stress and strain between individual grains, which confirms that the extreme models such as the static model and full constraint Taylor model can be ruled out for the present case. Therefore, for macroscopic texture simulations via VPSC, the α values of 0 and ∞ are not applicable.

Further information regarding the choice of the α parameter can be obtained by analysing the distribution of shear rates ($\dot{\gamma}_s$) on individual slip systems (s). A statistical parameter (T) related to the distribution of shear rates can be written as [40]

$$T = \frac{\sum_s (\dot{\gamma}_s)^2}{\left(\sum_s \dot{\gamma}_s\right)^2} \tag{9}$$

The theoretical maximum of the T parameter is 1, which corresponds to a single slip condition (static model), while the theoretical minimum is 0.125, which corresponds to equal distribution of shear rates on eight slip systems. Table 2 summarises the value of the T parameter for equal distribution of the shear rates on two, three, four, five, six, seven and eight slip systems.

For a typical case in which two slip systems are active, but the shear rates are not evenly distributed between the two slip systems, it can be easily envisioned that the T parameter will vary between 0.5 and 1, depending upon the skewness of the distribution. Similarly, the T parameter varies between 0.33 and 0.5 with an unequal distribution of the shear rates on three slip systems. In the case of an unequal distribution of the shear rates on four and five slip systems, a similar analogy can be extended to determine the range of the T parameter (Table 2). The advantage of performing DAMASK simulations is that information regarding the spatial distribution of shear rates can be easily obtained at each pixel of the representative volume element. Therefore, the range of the T parameter can be computed, which in turn can give an idea of the number of active slip systems.

The evolution of the average T parameter with strain is illustrated in Figure 5. It can be observed that the range of the T parameter is between $\sim$0.33 and 0.45, viz. unequal distribution of the shear rates on three slip systems. In the initial stages of rolling deformation (up to strain level of 0.2), there is some skewness in the distribution of shear rates, resulting in the T

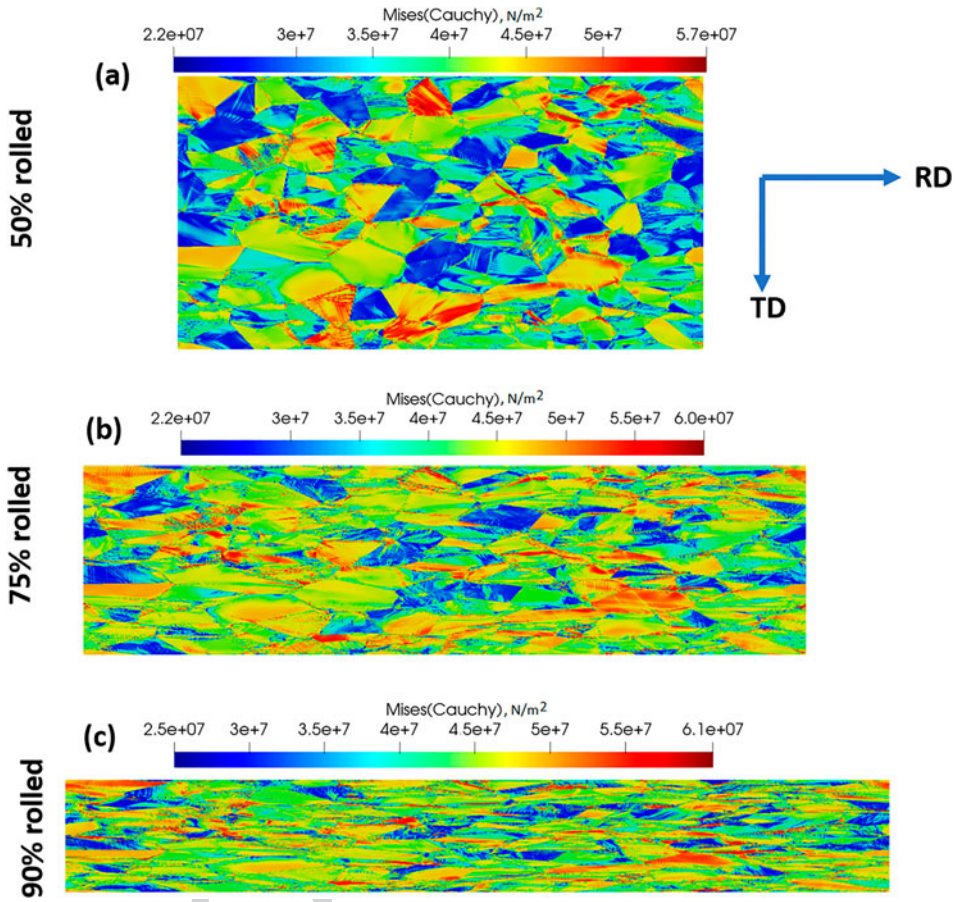

Figure 4. Spatial distribution of Von-Mises' equivalent stress after different rolling reductions: (a) 50% ($\varepsilon = 0.69$), (b) 75% ($\varepsilon = 1.4$) and (c) 90% ($\varepsilon = 2.7$).

Table 2. Values of the T parameter for equal and unequal distribution of shear rate on active slip systems.

Number of slip systems	T parameter for equal distribution of shear rate	T parameter for unequal distribution of shear rate
1	1	1
2	0.5	Between 0.5 and 1
3	0.33	Between 0.33 and 0.5
4	0.25	Between 0.25 and 0.33
5	0.2	Between 0.2 and 0.25
6	0.166	Between 0.166 and 0.2
7	0.142	Between 0.142 and 0.166
8	0.125	Between 0.125 and 0.142

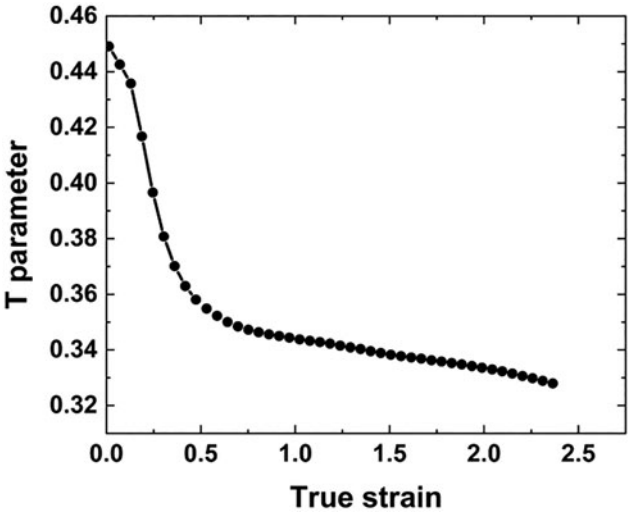

Figure 5. Evolution of the T parameter as a function of true strain during rolling deformation.

parameter varying around ~ 0.4. However, after intermediate rolling reductions (strain level of 0.6), the T parameter drops down nearly to 0.34–0.35. With further deformation, the T parameter decreases very slowly and reaches a value of 0.33 at a strain level of 2.3. This is a significant insight from DAMASK simulations as we now have some preliminary idea about the number of active slip systems in the material.

As mentioned previously, in VPSC simulations, the number of active slip systems is directly dependent upon the α parameter. Since we have some idea about the tentative number of active slip systems from DAMASK, the α parameter in VPSC can be decided in a fairly judicious manner. It has been observed by several researchers in the past that $\alpha = 0.1$ results on an average, three active slip systems for f.c.c. polycrystalline materials during rolling deformation. Therefore, to test the efficacy of the process, large-scale texture simulations were performed via VPSC with interaction parameter $\alpha = 0.1$. Based on the comparison between experimental and simulated ODF sections after 90% rolling reduction ($\varepsilon = -2.3$), the effectiveness of our approach can be established. Other details regarding

Colour online, B/W in print

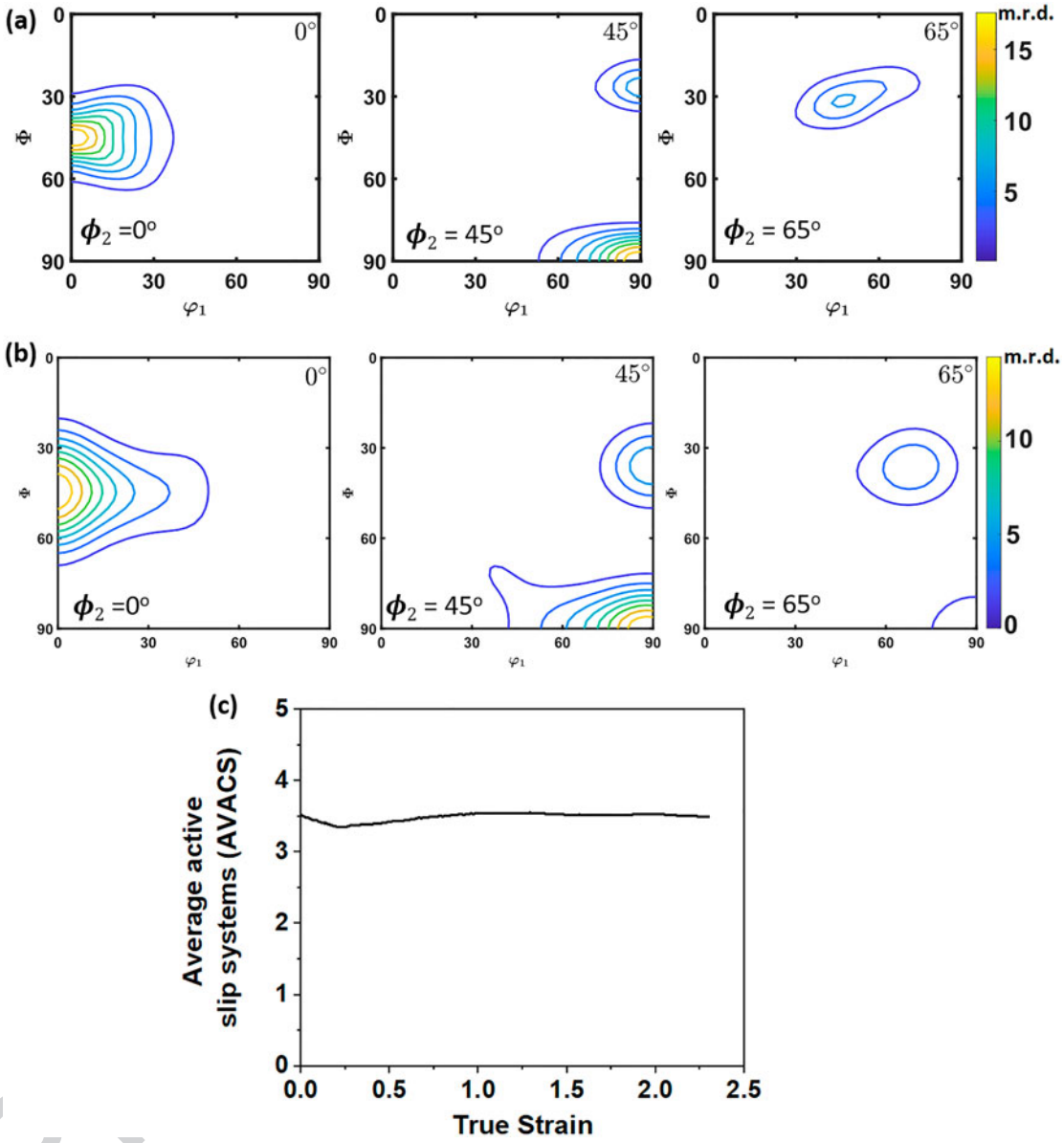

Figure 6. (a) Experimental ODF sections after 90% rolling, (b) simulated ODF sections after 90% rolling and (c) average number of active slip systems as a function of true strain during rolling deformation.

VPSC simulations such as strain increment, velocity gradient etc. are provided in the section 'Visco-plastic self-consistent simulations'.

Figure 6(a,b) shows the experimental and simulated ODF sections after 90% rolling reduction. It can be clearly observed that the main texture characteristics such as the strong α fibre connecting $\{110\}\langle001\rangle$ Goss and $\{110\}\langle1\bar{1}2\rangle$ brass components and the relatively weak $\{112\}\langle11\bar{1}\rangle$ copper and $\{123\}\langle63\bar{4}\rangle$ *S* components along the β fibre are satisfactorily reproduced by the simulations. The average number of active slip systems (AVACS $\sim$3–3.5) is illustrated in Figure 6(c), which confirms that learnings from the full-field model can be applied to the mean-field model for performing texture simulations in a judicious and transparent manner, rather than the previous approaches where the interaction parameter α was simply used as a fitting tool to achieve a good match with experimental textures.

Other simulation outputs such as texture and active slip systems at intermediate strain levels are provided in the supplementary file (Figure S1, Figure S2 and Table SI). With $\alpha = 0.1$, reasonable agreement between experiment and simulations can be observed at all levels of strain. For the sake of comparison, VPSC simulation results using other interaction schemes such as secant ($\alpha = 1$) and tangent ($\alpha = 0.05$) are also provided in the supplementary file (Figure S3). It can be clearly observed that these interaction schemes are not able to capture the experimental texture (Figure 6a) in a satisfactory manner.

Further insights regarding the general applicability of the proposed concept are obtained by performing DAMASK simulations on several ideal textures (copper, brass, *S*, cube, random) and different deformation modes (rolling, tension, shear). The average number of active slip systems was evaluated from DAMASK

based on the criteria proposed by Tome [25]. Figure S4 in the supplementary file shows that for a given set of hardening parameters, the number of active slip systems is weakly dependent on texture, whereas a strong dependency can be observed upon deformation mode. Therefore, it can be said that for a given deformation mode and hardening parameters, T parameter calculation and average slip system calculation from DAMASK can be extended to VPSC for any given texture. On the other hand, if the deformation mode is changed, there is a possibility of significant variation in the T parameter and average active slip systems. Therefore, fresh DAMASK simulations must be performed to determine the T parameter and the number of active slip systems, which can then be exported to the VPSC framework for performing bulk texture simulations.

In our future works, we aim to develop similar strategies where other learnings from DAMASK can be incorporated in the VPSC model. In particular, we aim to probe the effect of the local neighbourhood on the deformation response of individual grains in DAMASK so that a criterion for delineating strongly interacting and non-interacting grains can be established. Subsequently, this can be fed into the VPSC model in which the interacting grains can be paired together and made to co-rotate to empirically capture the role of local neighbourhood on texture evolution.

Summary

The important findings of the present work are summarised below:

(i) A pipeline where insight from the full-field DAMASK model is used in the mean-field VPSC model for performing large-scale texture simulations is established in the present work.
(ii) The value of the most critical parameter (α) in the localisation equation of VPSC can be determined in an elegant manner using the statistical criterion T parameter based on the distribution of shear rates at each material point in DAMASK. Subsequent texture simulations via VPSC provided an excellent match between experimental and simulated textures.
(iii) The DAMASK simulations highlighted that deformation condition is far off from the upper bound Taylor model and lower bound static model. Significant spatial variation in equivalent stress and equivalent strain was observed in the simulated microstructures.
(iv) The T parameter was observed to be varying between 0.45and 0.32 which indicated the operation of three slip systems. This information from DAMASK was used to choose the value of α as 0.1 for VPSC simualtions.
(v) The proposed approach is universal in nature and can be easily extended for different starting textures and microstructures.

Acknowledgements

The authors would like to thank Texture Lab, IIT Kanpur.

Disclosure statement

No potential conflict of interest was reported by the author(s).

Funding

There has been no financial support for this work.

References

[1] Bishop J, Hill R. CXXVIII. A theoretical derivation of the plastic properties of a polycrystalline face-centred metal. London, Edinburgh Dublin Philos Mag J Sci 1951;42(334):1298–1307.
[2] Bishop J, Hill R. XLVI. A theory of the plastic distortion of a polycrystalline aggregate under combined stresses. London, Edinburgh Dublin Philos Mag J Sci 1951;42(327):414–427.
[3] Hirsch J, Lücke K. Overview no. 76: mechanism of deformation and development of rolling textures in polycrystalline f.c.c. metals—I. Description of rolling texture development in homogeneous CuZn alloys. Acta Metall 1988;36(11):2863–2882.
[4] Hirsch J, Lücke K. Overview no. 76: mechanism of deformation and development of rolling textures in polycrystalline fcc metals—II. Simulation and interpretation of experiments on the basis of Taylor-type theories. Acta Metall 1988;36(11):2883–2904.
[5] Beyerlein I, Tomé C. A dislocation-based constitutive law for pure Zr including temperature effects. Int J Plast 2008;24(5):867–895.
[6] Van Houtte P. A comprehensive mathematical formulation of an extended Taylor–Bishop–Hill model featuring relaxed constraints, the Renouard–Wintenberger theory and a strain rate sensitivity model. Texture, Stress, Microstruct 1988;8:313–350.
[7] Mánik T, Holmedal B. Review of the Taylor ambiguity and the relationship between rate-independent and rate-dependent full-constraints Taylor models. Int J Plast 2014;55:152–181.
[8] Taylor GI. Plastic strain in metals. J Inst Met 1938;62:307–324.
[9] Kocks U, Chandra H. Slip geometry in partially constrained deformation. Acta Metall 1982;30(3):695–709.
[10] Van Houtte P. On the equivalence of the relaxed Taylor theory and the Bishop-Hill theory for partially constrained plastic deformation of crystals. Mater Sci Eng 1982;55(1):69–77.
[11] Molinari A, Canova G, Ahzi S. A self consistent approach of the large deformation polycrystal viscoplasticity. Acta Metall 1987;35(12):2983–2994.
[12] Lebensohn RA, Tomé C. A self-consistent anisotropic approach for the simulation of plastic deformation and texture development of polycrystals: application to zirconium alloys. Acta Metall Mater 1993;41(9):2611–2624.

[13] Van Houtte P, Li S, Seefeldt M, et al. Deformation texture prediction: from the Taylor model to the advanced Lamel model. Int J Plast 2005;21(3):589–624.
[14] Xie Q, Eyckens P, Vegter H, et al. Polycrystal plasticity models based on crystallographic and morphologic texture: evaluation of predictions of plastic anisotropy and deformation texture. Mater Sci Eng A 2013;581:66–72.
[15] Zhang K, Holmedal B, Hopperstad O, et al. Modelling the plastic anisotropy of aluminum alloy 3103 sheets by polycrystal plasticity. Modell Simul Mater Sci Eng 2014;22(7):075015.
[16] Tomé CN, Necker CT, Lebensohn RA. Mechanical anisotropy and grain interaction in recrystallized aluminum. Metall Mater Trans A 2002;33(8):2635–2648.
[17] Kanjarla AK, Van Houtte P, Delannay L. Assessment of plastic heterogeneity in grain interaction models using crystal plasticity finite element method. Int J Plast 2010;26(8):1220–1233.
[18] Liu B, Raabe D, Roters F, et al. Comparison of finite element and fast Fourier transform crystal plasticity solvers for texture prediction. Modell Simul Mater Sci Eng 2010;18(8):085005.
[19] Roters F, Eisenlohr P, Hantcherli L, et al. Overview of constitutive laws, kinematics, homogenization and multiscale methods in crystal plasticity finite-element modeling: theory, experiments, applications. Acta Mater 2010;58(4):1152–1211.
[20] Wronski M, Kumar MA, Capolungo L, et al. Deformation behavior of CP-titanium: experiment and crystal plasticity modeling. Mater Sci Eng A 2018;724:289–297.
[21] Canova G, Wenk H, Molinari A. Deformation modelling of multi-phase polycrystals: case of a quartz-mica aggregate. Acta Metall Mater 1992;40(7):1519–1530.
[22] Lebensohn RA. N-site modeling of a 3D viscoplastic polycrystal using fast Fourier transform. Acta Mater 2001;49(14):2723–2737.
[23] Kok S, Beaudoin AJ, Tortorelli DA. A polycrystal plasticity model based on the mechanical threshold. Int J Plast 2002;18(5-6):715–741.
[24] Molinari A, Tóth L. Tuning a self consistent viscoplastic model by finite element results—I. Modeling. Acta Metall Mater 1994;42(7):2453–2458.
[25] Tomé CN. Self-consistent polycrystal models: a directional compliance criterion to describe grain interactions. Modell Simul Mater Sci Eng 1999;7(5):723.
[26] Mishin VV, Shishov IA, Stolyarov ON, et al. Effect of cold rolling route on deformation mechanism and texture evolution of thin beryllium foils: experiment and VPSC simulation. Mater Charact 2020;164:110350.
[27] Roatta A, Leonard M, Nicoletti E, et al. Modeling texture evolution during monotonic loading of Zn-Cu-Ti alloy sheet using the viscoplastic self-consistent polycrystal model. J Alloys Compd 2021;860:158425.
[28] Kaushik L, Kim M-S, Singh J, et al. Deformation mechanisms and texture evolution in high entropy alloy during cold rolling. Int J Plast 2021;141:102989.
[29] Tazuddin BK, Gurao NP. Deciphering micromechanisms of plastic deformation in a novel single phase fcc-based MnFeCoNiCu high entropy alloy using crystallographic texture. Mater Sci Eng A 2016;657:224–233.
[30] Saleh AA, Haase C, Pereloma EV, et al. On the evolution and modelling of brass-type texture in cold-rolled twinning-induced plasticity steel. Acta Mater 2014;70:259–271.
[31] Saleh AA, Pereloma EV, Gazder AA. Microstructure and texture evolution in a twinning-induced-plasticity steel during uniaxial tension. Acta Mater 2013;61(7):2671–2691.
[32] Takajo S, Tomé CN, Vogel SC, et al. Texture simulation of a severely cold rolled low carbon steel using polycrystal modeling. Int J Plast 2018;109:137–152.
[33] Bachmann F, Hielscher R, Schaeben H. editors. Texture analysis with MTEX–free and open source software toolbox. Solid State Phenomena; 2010; Trans Tech Publ.
[34] Roters F, Diehl M, Shanthraj P, et al. DAMASK–The Düsseldorf Advanced Material Simulation Kit for modeling multi-physics crystal plasticity, thermal, and damage phenomena from the single crystal up to the component scale. Comput Mater Sci 2019;158:420–478.
[35] Diehl M, Groeber M, Haase C, et al. Identifying structure–property relationships through DREAM. 3D representative volume elements and DAMASK crystal plasticity simulations: an integrated computational materials engineering approach. JOM 2017;69(5):848–855.
[36] Diehl M, Wang D, Liu C, et al. Solving material mechanics and multiphysics problems of metals with complex microstructures using DAMASK—The Düsseldorf advanced material simulation kit. Adv Eng Mater 2020;22(3):1901044.
[37] Groeber MA, Jackson MA. DREAM. 3D: a digital representation environment for the analysis of microstructure in 3D. Integr Mater Manuf Innov 2014;3(1):56–72.
[38] Tomé C. Lebensohn R. VPSC 7b–User manual. 2007.
[39] Engler O, Hirsch J. Texture control by thermomechanical processing of AA6xxx Al–Mg–Si sheet alloys for automotive applications—a review. Mater Sci Eng A 2002;336(1):249–262.
[40] Delannay L, Kalidindi S, Van Houtte P. Quantitative prediction of textures in aluminium cold rolled to moderate strains. Mater Sci Eng A 2002;336(1-2):233–244.